19th Brazilian Congress of Thermal Sciences and Engineering
November 06th-10th, 2022, Bento Gonçalves - RS - Brazil

ENC-2022-0125
AMMONIA PRODUCTION FROM ENERGY USE OF OIL SLUDGE GASIFICATION

York Castillo Santiago
Leandro A. Sphaier
Karoline da Costa Rocha Fernandes Ferreira
Laboratory of Thermal Sciences (LATERMO), Department of Mechanical Engineering (TEM/PGMEC), Federal Fluminense University (UFF), Rua Passo da Pátria 156, Niterói, RJ, Brazil
yorkcastillo@id.uff.br; lasphaier@id.uff.br

Aldemar Martínez González
Centro de Innovación y Tecnología – Instituto Colombiano del Petróleo (ICP - Ecopetrol S.A). Gerencia de Desarrollo y Transferencia Tecnológica Km 7, vía Piedecuesta, Santander, Colombia
aldemar.martinez@ecopetrol.com.co

Abstract. *This paper focuses on the study of oil sludge (OS) gasification and the potential use of syngas produced for ammonia production. For this purpose, a computational gasification model was developed and validated to evaluate the influence of the air/steam mixtures as gasification agent on parameters such as cold gas efficiency, composition and low heating value (LHV) of syngas. The results show that as the gasification temperature rises, the volumetric fraction of* H_2 *increases to 24.9% at 1382 °C and then decreases to 21.5% at 1380, while the CO augmented as the gasification temperature rises. On the other hand, the syngas LHV ranged between 5 and 10* MJ/Nm^3 *for equivalence ratio higher than 0.3 and steam/OS ratio values between 0.5 and 1.5 kg steam/kg OS, indicating that a greater addition of gasification agent favored the reforming and thermal cracking reactions of the heavier organic fractions contained in OS. Subsequently, the produced syngas was used for ammonia synthesis, where 1.41 L* NH_3*/kg-OS was obtained at 30 bar. Based on the syngas properties, it is verified that heavy oil gasification could be a viable alternative that could efficiently transform a fuel from a refinery into add-value products.*

Keywords: *gasification, oil sludge, ammonia production, energy use*

1. INTRODUCTION

Both upstream and downstream operations in the oil industry can generate a lot of oily waste. Before the refining process, the oil is temporarily stored in tanks, where a considerable amount of heavy and light hydrocarbons tend to separate, while solid particles and water are generally associated with heavier hydrocarbons (Jafarinejad, 2016). This mixture of heavy organic fractions, solids, and water, mainly, is known as oil sludge (OS), which is removed during tank cleaning operations and later sent for treatment or final disposal (Johnson & Affam, 2019). As oil refining capacity increases, a greater amount of OS production is expected, with approximately 1.0 ton of this residue being generated for every 500 tons of oil processed, corresponding to 0.2% wt. (Martínez González et al., 2018).

The water, heavy metals, and polycyclic aromatic hydrocarbons (PAHs) content in OS composition favor the formation of a stable oil-water emulsion (Hu et al., 2020). Asphaltenes and resins could be responsible for the stability of the oil-water emulsion present in the OS since these components contain hydrophilic functional groups and, consequently, can act as lipophilic emulsifiers (Nezhdbahadori et al., 2018). On the other hand, the total petroleum hydrocarbons (TPH) content present in the oily waste can vary between 5% and 86% wt., while the water and solids content are in the range of 30-85% wt. and 5-46% wt., respectively (Hu et al., 2013).

Thus, the management and final disposal of OS generated during the oil refining process has received increasing attention due to its high concentration of PAHs and heavy metals recognized as hazardous waste in many countries (Egazar'yants et al., 2015). Various thermochemical conversion processes, such as pyrolysis, gasification, and incineration, have been proposed for the OS treatment due to can destroy the organic fractions of the waste and convert the inorganic fractions into stable ash or slag (Li et al., 2021).

Implementing systems based on the gasification process in oil refineries has great potential since it could be coupled to power cycles for heat and electricity generation, as well as other refinery processes for chemical products such as hydrogen and ammonia (Castillo Santiago et al., 2022). The gasification process transforms the carbonaceous compounds present in the feedstock into a syngas rich in hydrogen and carbon monoxide, where the chemical composition and heating value of the syngas depend on the raw material used, the operating conditions, the type of gasifier, as well as the gasification agent used (Hanchate et al., 2021). The most used types of gasification agents are air, oxygen, steam, or mixtures of air/steam and steam/oxygen, which determine the final characteristics of syngas, mainly in terms of the concentration of combustible gases, syngas yield, tar and sulfur content, among others (Sharma et al., 2021).

Recently, various OS gasification works have been developed, Chu et al. (2021) studied the OS gasification by varying temperature and steam/oil sludge (SOS) ratio. The H_2 yield maximum was 48.50 mL/min/g at 800 °C and SOS = 0.3:1, the char yield was greater than 50%, while the char particle size varied from 85 to 120 μm. The authors concluded that gasification is an efficient technology for OS treatment, which allows the energy recovery of petroleum wastes through the production of syngas and char. Castillo Santiago et al. (2021) assessed the OS gasification through a computational model considering three different gasification agents and studied the potential use of syngas to generate electricity using three power cycles (gas microturbine, steam Rankine cycle, and internal combustion engine). The results showed that a hydrogen-rich syngas (38.2 vol%) was produced using an air/steam mixture as gasification agent, and the highest energy recovery potential (0.47 kWh/kg-OS) was obtained from the configuration gasifier/internal combustion engine. Thus, OS gasification and the subsequent syngas use to generate electricity is a option to oily waste disposal. Likewise, Mazzoni et al. (2020) compared the plasma and entrained flow co-gasification of municipal-solid-waste and oily waste, obtaining a global efficiency of 41% when oxygen was used as gasification agent in plasma co-gasification system coupled to cycle combined power plant, but reaching 48% for the entrained flow gasifier/cycle combined configuration.

This work aims to study the gasification process for OS treatment and the subsequent use of syngas for ammonia production. Thus, a gasification simulation model was developed and validated, while different operational parameters and performance indexes such as gasification temperature, cold-gas efficiency, syngas composition and LHV were assessed. In order to determine the energy recovery potential from OS gasification, an assessment of syngas usage in an ammonia synthesis process was carried out, including a previous stage of the syngas reform aiming at the generation of rich-hydrogen gas fuel. Therefore, this approach provides information on OS thermochemical conversion into syngas and subsequent use in chemical product generation.

2. MATERIAL AND METHODS

To carry out the model of the OS gasification process, the process simulator Aspen HYSYS® v11.0 was selected, which could be used to mathematically model chemical processes, from unit operations to complete chemical plants and refineries. In order to simulate the mass stream in the process in Aspen HYSYS®, it is necessary to define them through the designation of chemical compounds available in the software database. Thus, Tab. 1 shows the chemical compounds considered for OS chemical characterization, which comprises a mixture of high molecular weight aromatic hydrocarbons, such as BTX (benzene, toluene, and xylene) and some compounds with 2 and 3 aromatic rings (Martínez González et al., 2019)

Table 1. Model components of oil sludge.

Component	Molar mass (kg/mol)	Fraction (%)
Benzene (C_6H_6)	18	10
Toluene (C_7H_8)	92	10
Naphthalene ($C_{10}H_8$)	128	10
Phenol (C_6H_6O)	94	10
Xylene (C_8H_{10})	106	10
Anthracene ($C_{14}H_{10}$)	178	5
Pyrene ($C_{16}H_{10}$)	202	5
Phenanthrene ($C_{14}H_{10}$)	178	5
Chrysene ($C_{18}H_{12}$)	228	5
Water (H_2O)	18	20
Sulfur (S)	32	1
Calcium oxide (CaO)	56	9

The schematic representation of the gasification process is shown in Fig. 1, where after being fed, the OS passes through a splitter in order to obtain two streams: one corresponding to the waste that will be sent to an oxidation process (combustion under stoichiometric conditions), while the other one refers to the amount of waste to be gasified (thermal decomposition under substoichiometric conditions), as shown by Eq. (1) and Eq. (2).

$$\left(\dot{m}_{os}\right)_{oxi} = \dot{m}_{os} \times X_{oxi} \tag{1}$$

$$\left(\dot{m}_{os}\right)_{gas} = \dot{m}_{os} \times \left(1 - X_{oxi}\right) \tag{2}$$

Where $\left(\dot{m}_{os}\right)_{oxi}$ is the OS mass flow rate to be oxidized (kg/h), $\left(\dot{m}_{os}\right)_{gas}$ the OS mass flow rate to be gasified (kg/h), $\dot{m}_{os}$ is the OS total mass flow rate (kg/h), while X_{oxi} is the OS fraction to be oxidized, separated in the splitter.

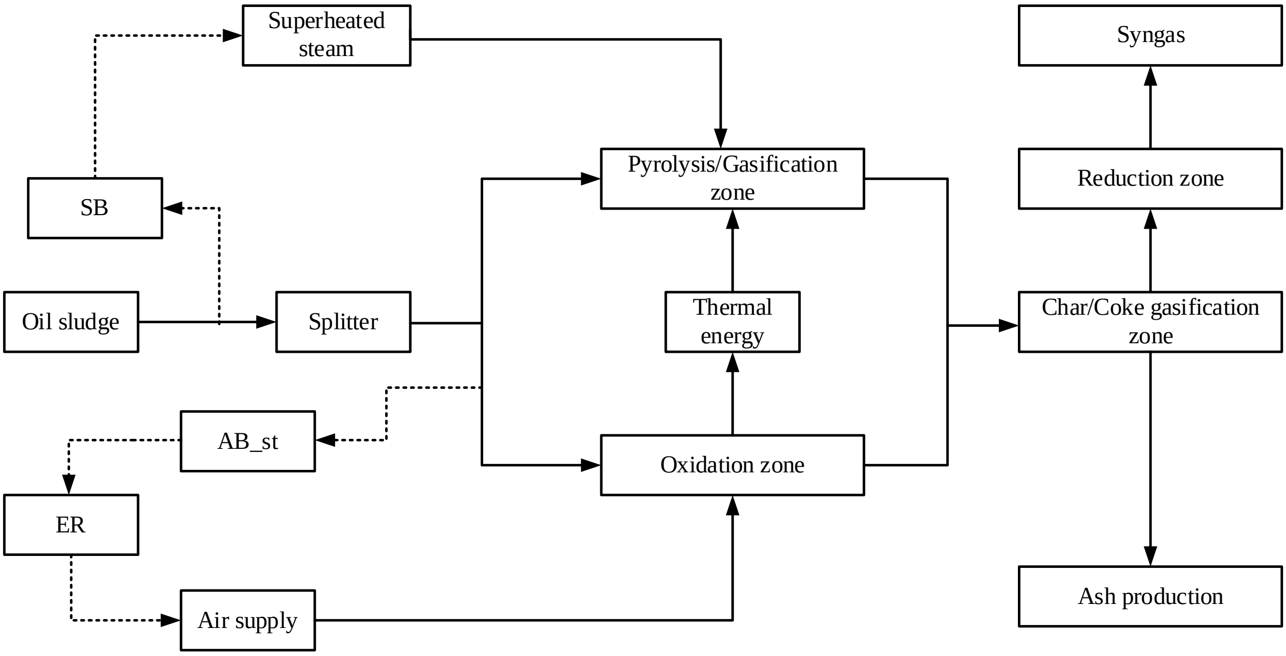

Figure 1. OS gasification scheme

Concerning gasification agents, a mixture of air and superheated steam was considered. The equivalence ratio (ER) was adopted for air supply, representing an input parameter in the proposed model, see Eq. (3).

$$ER = \frac{\left(\dot{m}_{air}\right)_f}{\left(\dot{m}_{air}\right)_{st}} = \frac{\left(\dfrac{\dot{m}_{air}}{\dot{m}_{OS}}\right)_f}{\left(\dfrac{\dot{m}_{air}}{\dot{m}_{OS}}\right)_{st}} = \frac{AB\_f}{AB\_st} \tag{3}$$

Where $\left(\dot{m}_{air}\right)_f$ is the mass flow of air supplied to the gasifier (kg/h), $\left(\dot{m}_{air}\right)_{st}$ the mass flow of stoichiometric air required in the OS oxidation (kg/h), (AB_st) the specific mass ratio of air supplied to the gasifier (kg/h), and (AB_f) specific mass ratio of stoichiometric air required in the OS oxidation (kg/h).

The total mass flow rate of air supplied to the OS process is calculated using Eq. (4), where AB_st and $\dot{m}_{OS}$ are used. Considering Eq. (5), it is possible to determine the $\left(\dot{m}_{air}\right)_{st}$, while the combination of Eqs. (4) and (5) result in Eq. (6), which allow concluding that both the ER and the stream separation fraction in the splitter (X_{oxi}) are equivalent.

$$\left(\dot{m}_{air}\right)_f = \left(AB\_f\right) \times \left(\dot{m}_{OS}\right)_{oxi} \tag{4}$$

$$\left(\dot{m}_{air}\right)_{st} = \left(AB\_st\right) \times \dot{m}_{OS} \tag{5}$$

$$ER = \frac{\left(\dot{m}_{air}\right)_f}{\left(\dot{m}_{air}\right)_{st}} = \frac{\left(AB\_f\right) \times \left(\dot{m}_{OS}\right)_{oxi}}{\left(AB\_st\right) \times \dot{m}_{OS}} = \frac{\left(\dot{m}_{OS}\right)_{oxi}}{\dot{m}_{OS}} = X_{oxi} \tag{6}$$

Therefore, ER could be defined as the mass fraction of OS to be oxidized in the thermochemical conversion process, as shown in Eq. (6).

The superheated steam supplied to the gasifier was calculated from the OS total mass flow and the steam/OS ratio (SB) supplied to the gasifier, as seen in Eq. (7). The SB ratio was defined as an input parameter in the present model, and it can vary between 0.5 and 1.5 kg steam/kg OS to guarantee mainly the char gasification, hydrocarbon reform, and Shift reactions (de Sales et al., 2017), (Gai et al., 2016).

$$SB = \frac{\dot{m}_{steam}}{\dot{m}_{OS}} \tag{7}$$

Where $\dot{m}_{steam}$ is the mass flow rate of superheated steam supplied to the gasifier (kg/h) and SB is the mass ratio of steam/petroleum OS (kg steam/kg OS).

For the simulation of the gasifier, four zones were defined, which cover the process of thermochemical conversion of the oily wastes: (i) oxidation zone, (ii) pyrolysis-gasification zone, (iii) char/coke gasification zone, and (iv) reduction zone, as indicated in Fig. 1. Once the air/steam mixture was used as a gasification agent, the thermal energy required in the pyrolysis-gasification endothermic reactions was supplied by the oxidation zone (exothermic reactions). Subsequently, the products derived from these two steps entered the char/coke gasification zone. The carbonaceous residues were converted into non-condensable gases such as CH_4, CO, CO_2, and H_2 through heterogeneous reactions. Thus, the gaseous products of this phase entered the reduction zone, where some homogeneous reactions occurred. Finally, two streams were produced in the gasifier: the syngas and a solid stream that corresponds to the ash and non-gasified carbon residues.

For the simulation of each step in the OS gasification process, some chemical reactions were considered, such as catalytic reforming with steam, thermal cracking, and partial oxidation, as well as their kinetic parameters in order to analyze the decomposition of the hydrocarbons present in the oily residue, as shown in Tab. 2.

Figure 2 shows the ammonia production scheme from syngas. Initially, OS from the refinery is treated to obtain syngas rich in hydrogen, methane, and carbon monoxide. Subsequently, the syngas is cleaned and sent to the reforming process, aiming to generate a gas with high hydrogen content. Finally, the hydrogen is separated from the syngas and mixed with atmospheric nitrogen (obtained from the separation of oxygen in the air) to be used in the ammonia synthesis. This alternative becomes relevant considering that synthetic ammonia corresponds to the main raw material for the production of fertilizers, mainly urea and ammonium nitrate (Alkusayer & Ollerhead, 2016). Therefore, synthetic ammonia could become one of the main products of the oil refinery with the potential to replace inputs or raw materials in the chemical industry. For the simulation of this case study, two later chemical processes are considered in the OS gasification process, which are (i) syngas reform and (ii) ammonia synthesis.

Table 2. Chemical reactions considered in the gasification model.

r_i	Chemical reaction name	Molar mass (kg/mol)	ΔH (kJ/mol)	Zone[a]
r_1	Phenol partial oxidation	$C_6H_6O + 4O_2 \rightarrow 6CO + 3H_2O$	-1300	O
r_2	Naphthalene partial oxidation	$C_{10}H_8 + 5O_2 \rightarrow 10CO + 4H_2$	-2200	O
r_3	Benzene partial oxidation	$C_6H_6 + 4.5O_2 \rightarrow 7CO + 4H_2$	-1500	O
r_4	Toluene partial oxidation	$C_7H_8 + 3.5O_2 \rightarrow 7CO + 4H_2$	-1800	O
r_5	Char partial oxidation	$2C + O_2 \rightarrow 2CO$	-110	CG
r_6	CO total oxidation	$2CO + O_2 \rightarrow 2CO_2$	-283	O
r_7	Hydrogen oxidation	$2H_2 + O_2 \rightarrow 2H_2O$	-240	O
r_8	Phenol thermic cracking	$C_6H_6O \rightarrow CO + 0.4\ C_{10}H_8 + 0.15\ C_6H_6 + 0.1CH_4 + 0.75H_2$	51	PG
r_9	Naphtalene thermic cracking	$C_{10}H_8 \rightarrow 6.5C + 0.5C_6H_6 + 0.1CH_4 + 1.5H_2$	-150	PG
r_{10}	Benzene reform	$C_6H_6 + 2H_2O \rightarrow 1.5C + 2.5CH_4 + 2CO$	-7.8	PG
r_{11}	Toluene reform	$C_7H_8 + 2H_2O \rightarrow 2C + 3CH_4 + 2CO$	-12	PG
r_{12}	Char hydrogenation	$C + 2H_2 \rightarrow CH_4$	-75	CG
r_{13}	Boudouard reaction	$C + CO_2 \rightarrow 2CO$	170	CG
r_{14}	Char gasification	$C + H_2O \rightarrow CO + H_2$	130	CG
r_{15}	$CaCO_3$ formation	$CaO + CO_2 \rightarrow CaCO_3$	-170	O/CG
r_{16}	Methane reforming	$CH_4 + H_2O \leftrightarrow CO + 3H_2$	206	R
r_{17}	Shift reaction	$CO + H_2O \leftrightarrow H_2 + CO_2$	-41	R

([a]) Gasifier zones. O: oxidation, PG: pyrolysis/gasification, CG: Char/Coke gasification, R: reduction.

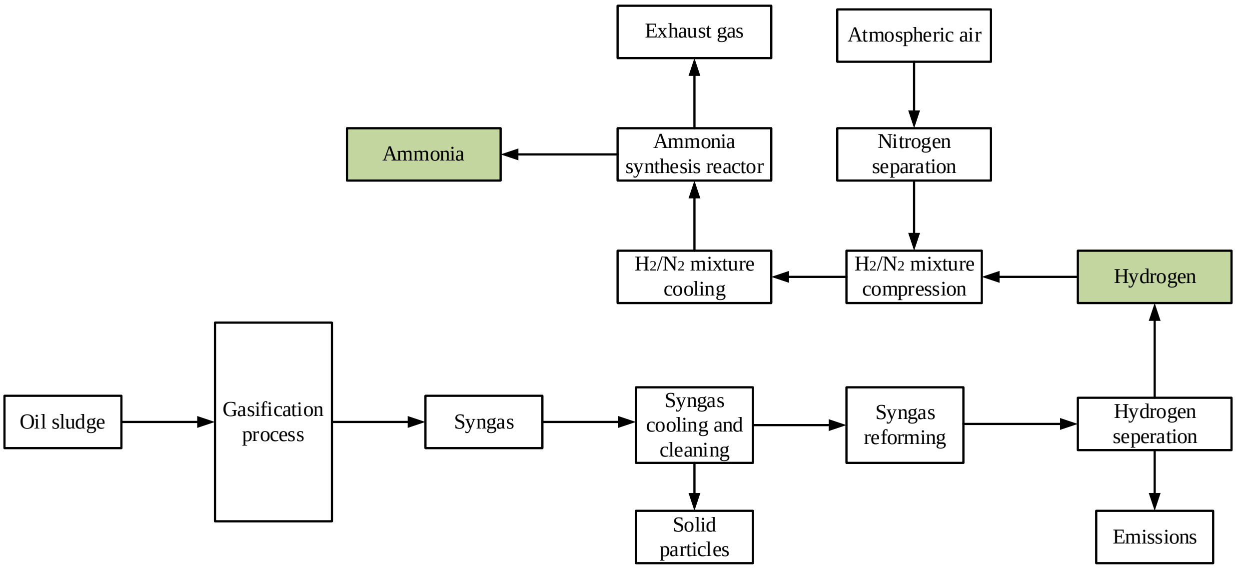

Figure 2. Ammonia synthesis scheme

To validate the gasification model, Orimulsion® (oil with API grade around 8 and moisture content of 30% wt.) was considered as feedstock. Thus, Tab. 3 shows the operating conditions of gasifier and the main properties of the feedstock to be gasified.

Subsequently, a comparative analysis was carried out between the main results obtained through the simulation model proposed in this study and the results reported by Ashizawa et al. (2005), which work was used as the reference to validation, as presented in Tab. 4. Additionally, the deviation between model results and the experimental data was quantified through the root mean square (RMS) error. It is worth noting that the difference between the LHV reported in Table 4 is mainly due to the difference between the CH_4 content, which is the chemical compound with the greatest influence on the syngas calorific value on a volumetric basis.

Table 3. Orimulsion® ultimate and proximate analysis to model validation (Ashizawa et al., 2005).

Parameter	Value/description	Unit
Ultimate analysis		
Carbon	84.28	%
Hydrogen	10.33	%
Oxygen	0.55	%
Nitrogen	0.64	%
Sulfur	3.95	%
Proximate analysis		
Moisture	28.80	%
Ash	0.18	%
Carbon fixed	12.84	%
Volatile	55.37	%

Table 4. Model validation comparison

Property	(Ashizawa et al., 2005)	This work	Absolut error (-)	Relative error (%)	RMS
CO (% vol.)	38.7	40.57	0.93	2.36	2.83
CO_2 (% vol.)	8.67	8.71	0.02	0.23	
H_2 (% vol.)	39.4	45.64	3.12	7.34	
CH_4 (% vol.)	0.08	1.96	0.94	32.16	
Others (% vol.)	0.38	0.27	0.05	16.92	
LHV (MJ/Nm^3)	9.7	11.1	0.70	6.73	
Process temp (°C)	1265	1292	41	3.14	

3. RESULTS AND DISCUSSION

3.1 Gasification process

Figure 3 shows the increasing behavior of the gasification temperature as the equivalence ratio ER increases, while the greater availability of oxygen promotes the oxidation reactions. However, the progressive injection of superheated steam as a gasification agent into the reactor tends to decrease the internal temperature of the process (Hernández et al., 2012). According to the results obtained from the simulation, it is observed that for an ER=0.30 and an SB=0.5 kg steam/kg OS, the gasification temperature reached is around 1300 °C, while for SB values of 1.0 and 1.5 kg steam/kg OS, the temperature decreases to 980 °C and 800 °C, respectively.

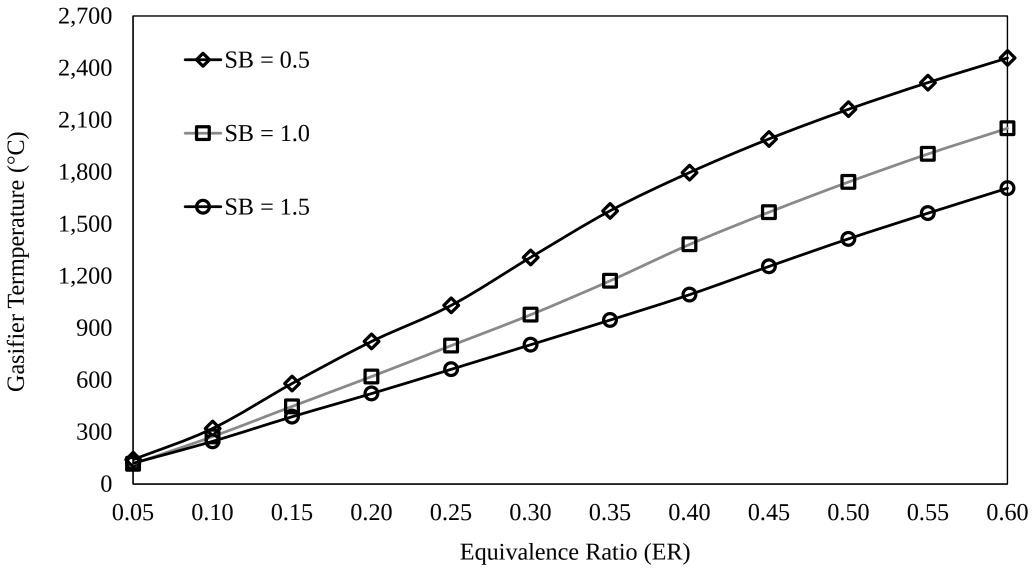

Figure 3. Gasification temperature for different ER values.

Figure 4 shows the expected composition of syngas obtained from OS thermochemical conversion. It is observed that the increase in temperature favors the reactions of thermal cracking and steam reforming, reducing the concentration of CxHy, although the highest molar concentration of H_2, CO, and CH_4 in the syngas obtained in the temperatures range between 1200-1400 °C. H_2 fraction increases and reaches a maximum value of 24.8% at a temperature of 1380 °C and then decreases, which is associated with the shift and char hydrogenation reactions (exothermic), so temperatures greater than 600 °C favor the formation of the reactants of these reactions (Van Huynh, 2011).

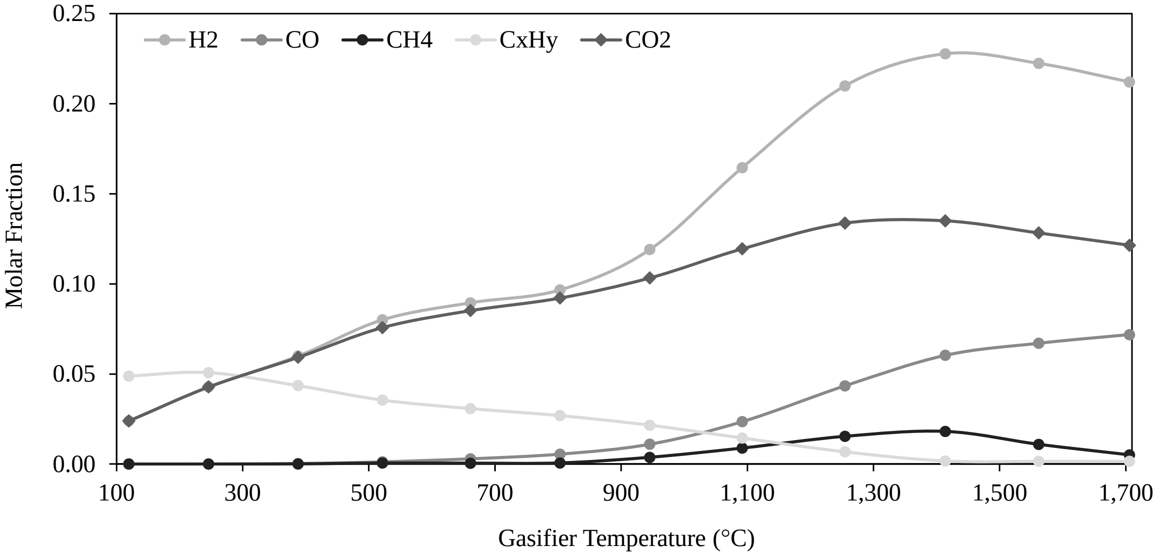

Figure 4. Syngas composition for different gasification temperatures

Regarding syngas LHV, a decreasing trend was observed as the ER was increased until reaching a value that oscillated in the range of 5 and 10 MJ/Nm^3 for ER>0.30 and SB between 0.5 and 1.5 kg steam/kg OS. This could be associated with the steam supply into the gasifier, which favored the thermal cracking of the heavier organic fractions in the OS, producing lighter hydrocarbons with lower energy content and consequently a mixture of less dense combustible gases with minor LHV (Kumar et al., 2009). The results showed that for an ER=0.3 and SB=0.5, the syngas LHV was 8.6 MJ/Nm^3, however, the LHV decreased to 6.7 MJ/ Nm^3 when the steam ratio was 1.5 kg steam/kg OS, as shown in Fig. 5.

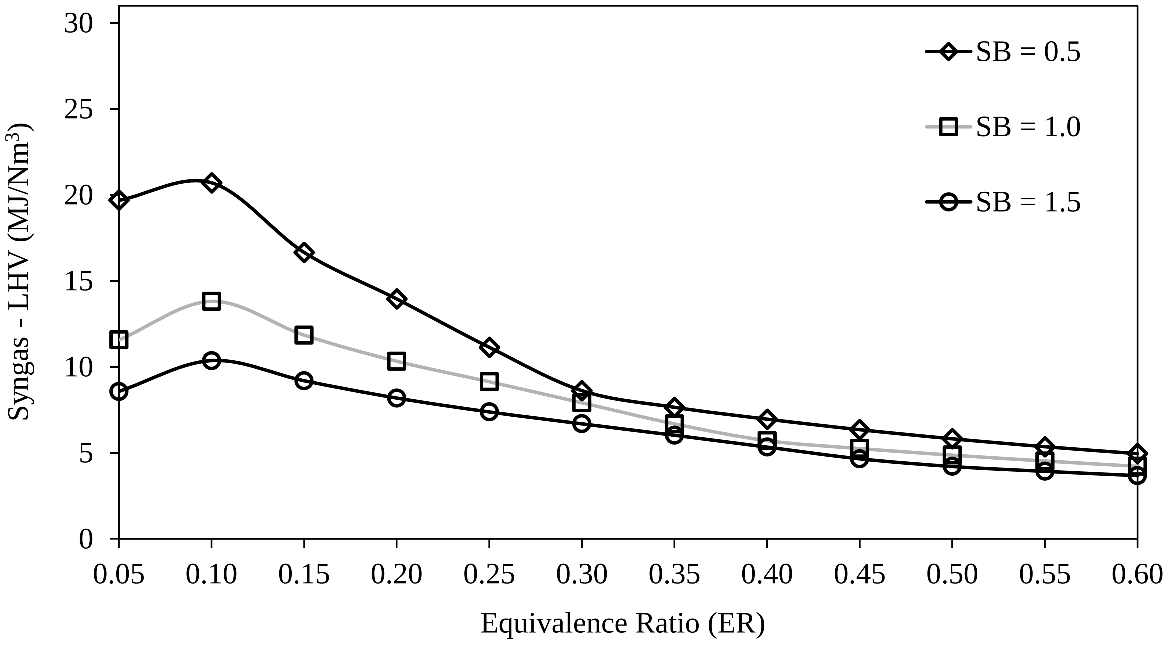

Figure 5. Syngas LHVfor different ER values

Figure 6 shows a decreasing trend in cold efficiency as the ER equivalence ratio increases, with the presence of oxygen and nitrogen favoring the oxidation reactions and the dilution effect, respectively. Thus, the combustible gas content in the syngas is reduced, and consequently, the cold efficiency decreases from 80% to 65% approximately.

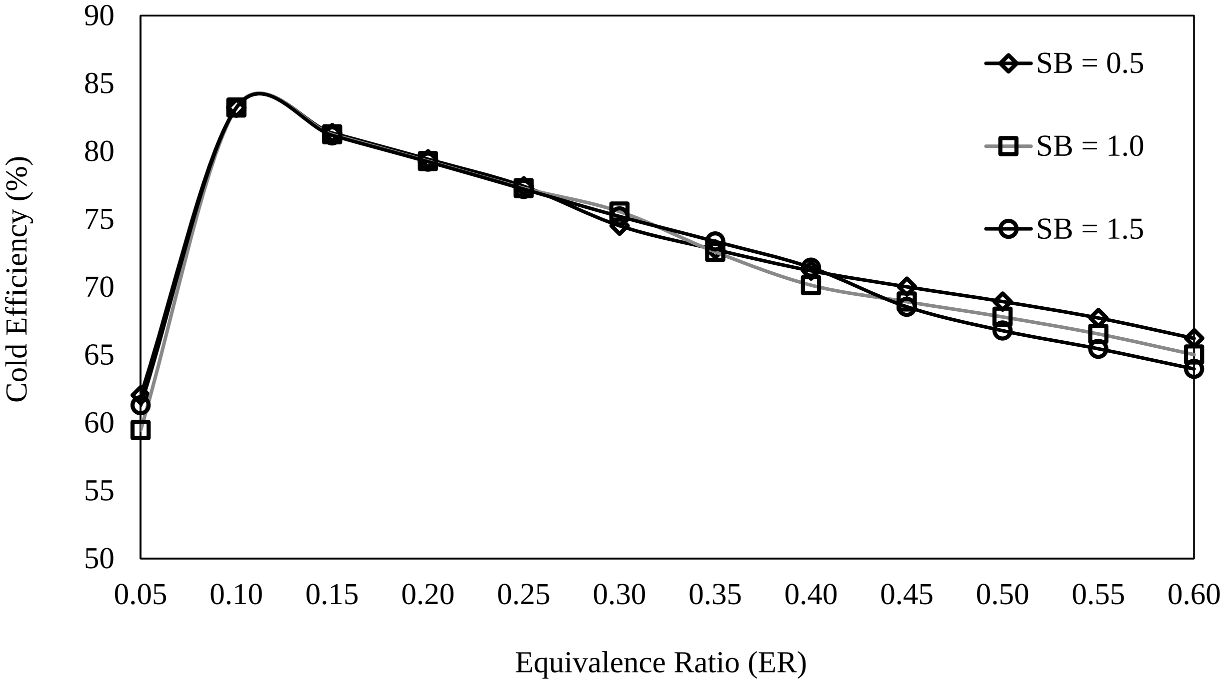

Figure 6. Cold gas efficiency for different ER values

3.2 Ammonia production

For ammonia production, it is worth noting that the ammonia synthesis reaction does not occur at room temperature because nitrogen requires a considerable amount of thermal energy to dissociate, which occurs at temperatures above 2,000 °C approximately (Bicer et al., 2016). Thus, an increase in the temperature of the reactants would be necessary, however, the inverse reaction of the ammonia synthesis becomes predominant due to its exothermic nature, where the chemical equilibrium is shifted towards the formation of H_2/N_2 instead of ammonia in agreement with Le Châtelier's principle. Therefore, the presence of a catalyst iron-base becomes indispensable to reduce the reaction temperature and favor chemical equilibrium without compromising the reaction rate (Modak, 2002).

Figure 7 shows the results of specific ammonia production as a function of the operating pressure flash separator after the synthesis reaction. Thus, an ammonia production rate of around 1.41 L/kg OS is expected, particularly for pressures above 30 bar in the flash separator, where the ammonia condensation temperature is approximately 21°C. Considering a mass flow of 1,000 kg/h BO in the gasification process, a potential ammonia production of 12.35 m^3/year is estimated.

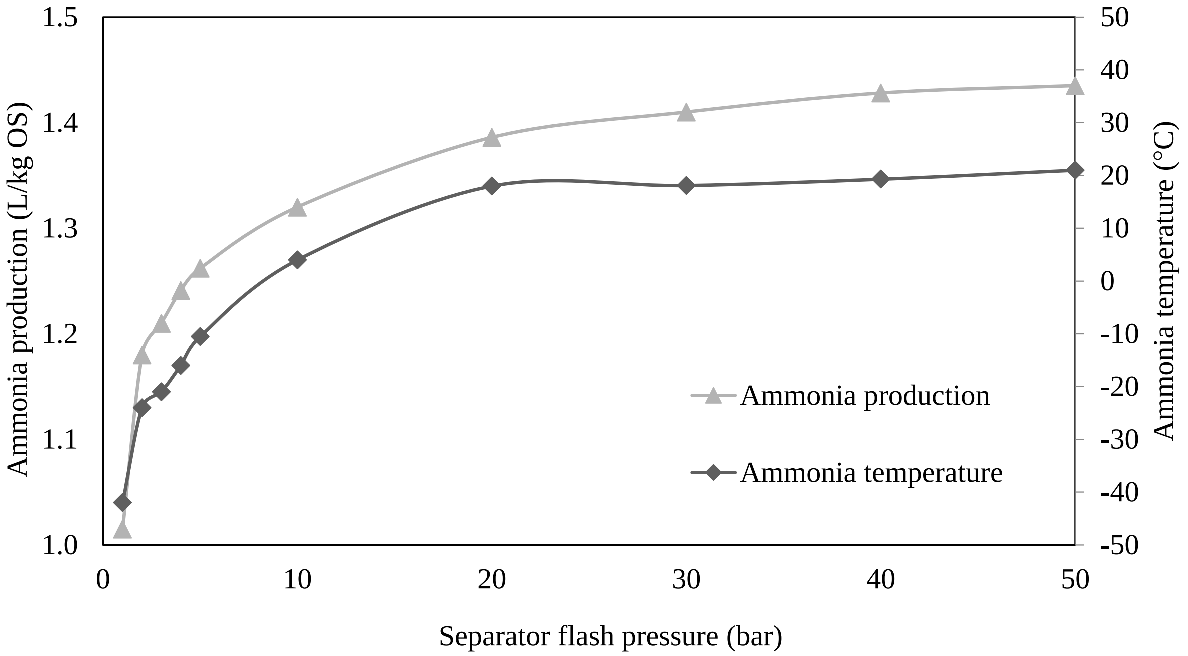

Figure 7. Specific ammonia production for different pressures of separator flash

4. CONCLUSIONS

The present work studied the possibility of using solid residues from the oil refinery, particularly OS and its thermochemical conversion into chemical products. According to the results obtained, it is concluded that the mixtures of air and superheated steam (as gasification agent) lead to the obtaining of syngas with high energy content, considering the ER and SB ratio in the range of 0.25-0.37 and 0.5-1.5 kg steam/kg OS, respectively. Under these conditions, syngas can be obtained with a molar concentration of H_2 around 10-25% and an LHV between 7.0 - 11.1 MJ/Nm^3.

In general terms, it is concluded that the increase in the gasification temperature favors the reactions of thermal cracking and steam reforming for hydrocarbons (CxHy), leading to a higher molar concentration of H_2, CO, and CH_4 in the syngas. Regarding ammonia production, it is observed that a synthetic ammonia specific production index of approximately 1.41 L NH_3/kg OS can be obtained. For this process, it could also be concluded that the increase in the operating pressure above 30 bar in the ammonia synthesis reactor does not lead to a representative augment in the ammonia production index.

Finally, the OS gasification process study showed the potential of the thermochemical conversion route and energy recovery of oily residues from the oil refineries, which could become promising technological alternatives for OS treatment before its final disposal.

5. ACKNOWLEDGEMENTS

The authors wish to express their gratitude for the financial support provided by CNPq, CAPES, FAPERJ, and the Human Resources Program of the ANP (PRH-ANP 51.1).

6. REFERENCES

Alkusayer, K. T., & Ollerhead, A. (2016). *Ammonia Synthesis for Fertilizer Production*. Worcester Polytechnic Institute.

Ashizawa, M., Hara, S., Kidoguchi, K., & Inumaru, J. (2005). Gasification characteristics of extra-heavy oil in a research-scale gasifier. *Energy*, *30*(11-12 SPEC. ISS.), 2194–2205.

Bicer, Y., Dincer, I., Zamfirescu, C., Vezina, G., & Raso, F. (2016). Comparative life cycle assessment of various ammonia production methods. *Journal of Cleaner Production*, *135*, 1379–1395.

Castillo Santiago, Y., Martínez González, A., Venturini, O. J., Sphaier, L. A., & Ocampo Batlle, E. A. (2022). Energetic and environmental assessment of oil sludge use in a gasifier/gas microturbine system. *Energy*, *244*, 123103.

Castillo Santiago, Y., Martínez González, A., Venturini, O. J., & Yepes Maya, D. M. (2021). Assessment of the energy recovery potential of oil sludge through gasification aiming electricity generation. *Energy*, *215*, 119210.

Chu, Z., Gong, Z., Wang, Z., Zhang, H., Liu, L., Wu, J., & Wang, J. (2021). Experimental study on gasification of oil sludge with steam and its char characteristic. *Journal of Hazardous Materials*, *416*, 125713.

de Sales, C. A. V. B., Maya, D. M. Y., Lora, E. E. S., Jaén, R. L., Reyes, A. M. M., González, A. M., Andrade, R. V., & Martínez, J. D. (2017). Experimental study on biomass (eucalyptus spp.) gasification in a two-stage downdraft reactor by using mixtures of air, saturated steam and oxygen as gasifying agents. *Energy Conversion and Management*, *145*, 314–323.

Egazar'yants, S. V, Vinokurov, V. A., Vutolkina, A. V, Talanova, M. Y., Frolov, V. I., & Karakhanov, E. A. (2015). Oil Sludge Treatment Processes. *Chemistry and Technology of Fuels and Oils*, *51*(5), 506–515.

Gai, C., Guo, Y., Liu, T., Peng, N., & Liu, Z. (2016). Hydrogen-rich gas production by steam gasification of hydrochar derived from sewage sludge. *International Journal of Hydrogen Energy*, *41*(5), 3363–3372.

Hanchate, N., Ramani, S., Mathpati, C. S., & Dalvi, V. H. (2021). Biomass gasification using dual fluidized bed gasification systems: A review. *Journal of Cleaner Production*, *280*, 123148.

Hernández, J. J., Aranda, G., Barba, J., & Mendoza, J. M. (2012). Effect of steam content in the air–steam flow on biomass entrained flow gasification. *Fuel Processing Technology*, *99*, 43–55.

Hu, G., Feng, H., He, P., Li, J., Hewage, K., & Sadiq, R. (2020). Comparative life-cycle assessment of traditional and emerging oily sludge treatment approaches. *Journal of Cleaner Production*, *251*, 119594.

Hu, G., Li, J., & Zeng, G. (2013). Recent development in the treatment of oily sludge from petroleum industry: A review. *Journal of Hazardous Materials*, *261*, 470–490.

Jafarinejad, S. (2016). Petroleum waste treatment and pollution control. In S. Jafarinejad (Ed.), *Petroleum Waste Treatment and Pollution Control* (1st ed.). Elsevier Inc.

Johnson, O. A., & Affam, A. C. (2019). Petroleum sludge treatment and disposal: A review. *Environmental Engineering Research*, *24*(2), 191–201. https://doi.org/10.4491/eer.2018.134

Kumar, A., Jones, D. D., & Hanna, M. A. (2009). Thermochemical Biomass Gasification: A Review of the Current Status of the Technology. *Energies*, *2*, 556–581.

Li, J., Lin, F., Li, K., Zheng, F., Yan, B., Che, L., Tian, W., Chen, G., & Yoshikawa, K. (2021). A critical review on energy recovery and non-hazardous disposal of oily sludge from petroleum industry by pyrolysis. *Journal of Hazardous Materials*, *406*, 124706.

Martínez González, A., Silva Lora, E. E., & Escobar Palacio, J. C. (2019). Syngas production from oil sludge gasification and its potential use in power generation systems: An energy and exergy analysis. *Energy*, *169*, 1175–1190.

Martínez González, A., Silva Lora, E. E., Escobar Palacio, J. C., & Almazán del Olmo, O. A. (2018). Hydrogen production from oil sludge gasification/biomass mixtures and potential use in hydrotreatment processes. *International Journal of Hydrogen Energy*, *43*(16), 7808–7822.

Mazzoni, L., Janajreh, I., Elagroudy, S., & Ghenai, C. (2020). Modeling of plasma and entrained flow co-gasification of MSW and petroleum sludge. *Energy*, *196*, 117001.

Modak, J. M. (2002). Haber process for ammonia synthesis. *Resonance*, *7*(9), 69–77.

Nezhdbahadori, F., Abdoli, M. A., Baghdadi, M., & Ghazban, F. (2018). A comparative study on the efficiency of polar and non-polar solvents in oil sludge recovery using solvent extraction. *Environmental Monitoring and Assessment*, *190*(7), 389.

Sharma, P., Gupta, B., Pandey, M., Singh Bisen, K., & Baredar, P. (2021). Downdraft biomass gasification: A review on concepts, designs analysis, modelling and recent advances. *Materials Today: Proceedings*, *46*, 5333–5341.

Van Huynh, C. (2011). *Performance characterization of a pilot-scale oxygen enriched-air and steam blown gasification and combustion system*. Iowa State University.

7. RESPONSIBILITY NOTICE

The authors are the only ones responsible for the printed material included in this paper.